24th COBEM - 2017

24th ABCM International Congress of Mechanical Engineering
December 3-8, 2017, Curitiba, PR, Brazil

COBEM-2017-2073
A COMPARISON BETWEEN COMPOSITE ROTORDYNAMICS MODELING THEORIES

Paulo Costa Porto de Figueiredo Barbosa
Vergílio Torezan Silingardi Del Claro
Aldemir Ap Cavalini Jr
Valder Steffen Jr
LMEst - Laboratory of Mechanics and Structures, Federal University of Uberlândia, School of Mechanical Engineering, Av. João Naves de Ávila, 2121, Uberlândia, MG, 38408-196, Brazil.
paulo.barbosa@ufu.br, vergilio.claro@ufu.br, aacjunior@ufu.br, vsteffen@ufu.br.

Abstract. *Various applications of composite materials have been prominent in recent years, given their many advantages over the equivalent conventional engineering materials counterparts. Following this tendency, rotating machinery in general are now being improved with the substitution of metallic shafts by composite ones, resulting greater operation speeds, lower overall weight and better structural efficiency, among other aspects. In this sense, some models have been proposed for the computational modelling of rotating machinery with composite shafts. A comparison between simplified beam models for composite shafts is presented in this contribution. Also, an experimental validation of the implemented models is carried out in terms of the frequency response functions for the free-free condition. The rotor critical speeds, vibration amplitudes, transient motion, and instability thresholds were numerically determined.*

Keywords: *shaft, composite, numerical models.*

1. INTRODUCTION

Composite materials can be defined as a system constituted by two or more phases in macroscopic scale (Daniel and Ishai, 1994). The use of composite materials has grown over the years, which is associated to the range of possibilities in obtaining suitable mechanical characteristics for each application. Composite materials are being broadly introduced in rotating machines over the recent years (Silveira, 2001). In subcritical operating conditions, it is interesting to decrease weight and maximize the torque transmission for many applications, such as *cardan* shafts for the automotive industry. The low weight of composite shafts allows for high acceleration rates (Brush, 1999), which is ideal for a considerable range of engineering applications. In supercritical conditions, some additional factors, such as bending vibration, dynamic strain variation, stability, and fatigue, must be considered (Gupta, 2015).

The fabrication techniques of composite material components are evolving rapidly, enabling great customization and very specific layers configurations. The layers constituting composite shafts can be adjusted to modify their mechanical properties, thus changing the critical speeds according to the operational speed or obtaining smooth run-up and run-down profiles (Pereira and Swider, 1997). This is interesting for complex applications, since it allows precise and optimized design in various situations. All these points increase the complexity of the models needed to represent this composite material shafts. Other effects, such as structural damping, can reduce vibration amplitudes in critical speeds, but also may lead to instability (Silveira, 2001). The internal damping of composite shafts can be two times bigger than the one associated with metallic shafts (Wattergreen and Olsson, 1996).

Therefore, the characterization of composite shafts presents fundamental importance on rotating machinery design, especially for supercritical rotors to guarantee safety operating conditions. Nevertheless, determining the composite shaft physical parameters that allow for an accurate instability prediction can be difficult (Sino, 2007).

In the present contribution, different numerical models are compared regarding their ability to predict the dynamic behavior of a composite shaft. The shaft considered is a simple thick-walled shaft, with twenty layers of different orientations and thicknesses, being the last external layer a special crisscrossed layer of 0/90º fiber orientation. The material of the shaft fibers is plain weave carbon fiber, with the exception of the external layer, embedded in an epoxy resin matrix. Some emphasis is given to the model's ability to properly represent the composites damping, since it has been proven difficult to be described (Wettergren, 1997; Singh and Gupta, 1994).

2. ROTOR MODEL

The numerical model of the rotor was developed using finite elements theories, on Matlab® environment, based on beam elements with eight degrees-of-freedom, as showed in Fig. 1. Equation (1) presents the differential equation that represents the dynamic behavior of a flexible rotor system operating in a steady state condition (Lalanne and Ferraris, 1998).

$$\boldsymbol{M}\,\ddot{\boldsymbol{\delta}} + \left[\,\boldsymbol{D} + \Omega\,\boldsymbol{D}_{\boldsymbol{g}}\,\right]\dot{\boldsymbol{\delta}} + \boldsymbol{K}\,\boldsymbol{\delta} = \boldsymbol{W} + \boldsymbol{F}_{\boldsymbol{u}} \tag{1}$$

where $\boldsymbol{M}$ is the mass matrix, $\boldsymbol{D}$ is the damping matrix (e.g., associated with the bearings), $\boldsymbol{D}_g$ represents the gyroscopic effect, and $\boldsymbol{K}$ is the stiffness matrix. The vector $\boldsymbol{\delta}$ contains the generalized displacements (i.e., the lateral vibrations of the shaft), and Ω is the shaft rotation speed. $\boldsymbol{W}$ stands for the weight of the rotating parts and $\boldsymbol{F}_u$ represents the unbalance forces.

Considering the dissipative effects associated of composite materials (Sino, 2007), Eq. (1) is them modified as follows:

$$\boldsymbol{M}\,\ddot{\boldsymbol{\delta}} + \left[\,\boldsymbol{D} + \Omega\,\boldsymbol{D}_{g} + \boldsymbol{D}_{i}\,\right]\dot{\boldsymbol{\delta}} + \left[\boldsymbol{K} + \Omega\boldsymbol{K}_{i}\right]\boldsymbol{\delta} = \boldsymbol{W} + \boldsymbol{F}_{u} \tag{2}$$

where $\boldsymbol{D}_i$ and $\boldsymbol{K}_i$ are the internal damping and the stiffness matrices, respectively, both associated with the composite material.

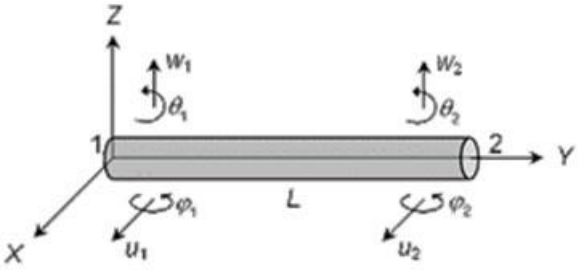

Figure 1. Beam element with 8 degrees-of-freedom

2.1 Composite Shaft

For the numerical simulation of the rotor with a composite hollow shaft, simplifying hypothesis are used. In this paper, two different simplified beam models were used to determine the parameters associated with the composite shaft. A comparison between them will be presented in the following.

2.1.1 Equivalent Modulus Beam Theory (EMBT)

Presented by Singh and Gupta (1996), the EMBT model essentially determines an equivalent Young modulus E_{eq}, as presented in Eq. (3), and the shear modulus G_{eq} of Eq. (4).

$$E_{eq} = \frac{4(U_1 - U_5)(U_1 - U_3\gamma) - \beta^2 U_2^2}{U_1 - \beta U_2 + \gamma U_3} \qquad \text{where} \qquad \gamma = \sum_{k=1}^{N} \frac{t_k}{t}\cos 4\theta_k \quad \beta = \sum_{k=1}^{N} \frac{t_k}{t}\cos 2\theta_k \tag{3}$$

$$G_{eq} = U_5 - U_3\gamma \tag{4}$$

in which t_p is the thickness of the ply k, t is the thickness of the composite shaft, θ_k is the angular direction of the fibers of the ply k, and N is the number of plies. U_1, U_2, U_3, and U_5 are laminate invariants showed in Daniel and Ishai (1994).

2.1.2 Simplified Homogenized Beam Theory (SHBT)

Presented by Sino (2007), the SHBT model considers a homogenized flexural stiffness with Young's modulus E_y^k and inertia moment of area I_k for each ply, as shown in Eq. (5).

$$EI = \sum_{k=1}^{N} E_y^k I^k \qquad where \qquad I^k = \frac{\pi}{4}(R_k^4 - R_{k-1}^4)$$

$$E_y^k(\theta) = \frac{1}{\frac{c^4}{E_l} + \frac{s^4}{E_t} + c^2 s^2 \left(\frac{1}{G_{lt}} - 2\frac{\upsilon_{lt}}{E_t} \right)} \tag{5}$$

in which R_{p-1} and R_p are is the inner radius and outer radius associated with the ply k, respectively. The angular direction of the fibers is given by θ, where s represents $sin(\theta)$ and c represents $cos(\theta)$. E_l and E_t are the longitudinal and transversal Young's modulus, respectively, associated with each ply k. G_{it} is the shear modulus and v_{it} is the Poisson's ratio.

2.1.3 Internal Damping

The internal damping associated with the composite hollow shaft is modeled as a viscous damping, which depends on the expression $EI\eta$, where η is the loss factor. This is derived from the Kelvin-Voigt model (Sino, 2007). The parameter η is determined by solving a typical inverse problem by using the Differential Evolution heuristic optimization technique (Storn and Price, 1995).

3. EXPERIMENTAL RESULTS

The composite hollow shaft used in the experimental analysis is showed in Fig. 2a. It is manufactured from a special high-modulus pre-impregnated carbon fiber ply and has twenty layers with the following stacking sequence: [0 0 0 0 90 90 45 -45 0 0 0 45 -45 90 90 0 0 0 0 0/90] (see Fig. 2b). Table 1 summarizes the physical and geometric properties of the composite shaft used in the present work provided by the manufacturer.

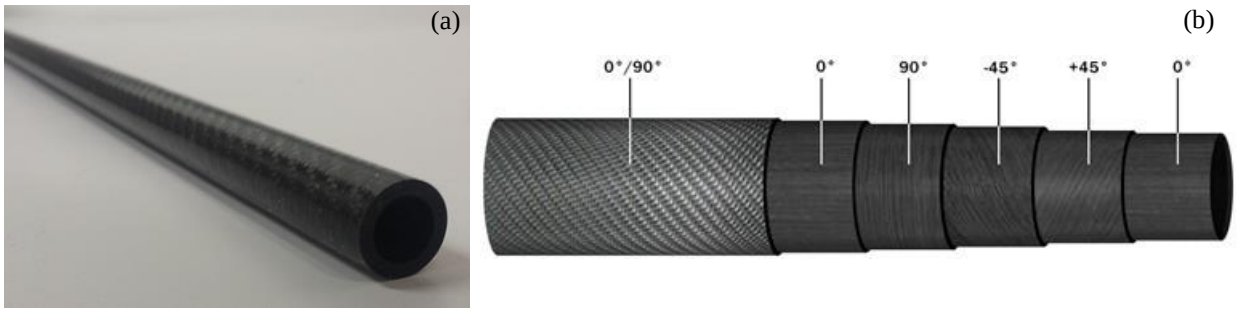

Figure 2. Composite hollow shaft

Table 1. Properties of the analyzed composite shaft provided by the manufacturer.

Properties	Value
Length (m)	0.907
Outer diameter (m)	0.018
Internal diameter (m)	0.0128
Density (kg/m3)	1600
Young's Modulus 0° (GPa)	90,70
Young's Modulus 90° (GPa)	68,50
In-Plane Shear Modulus (GPa)	11,25
Major Poisson's Ratio	0.38

Frequency response functions (FRFs) were obtained for the free-free condition of the composite hollow shaft by performing an impact hammer modal analysis. Impact forces were applied at L=0.378m along the horizontal direction and the vibration responses were measured by accelerometers installed at the positions L=0m, L=0.378m and L=0.529m along the same direction of the impact forces, as exemplified in Fig. 3.

Therefore, both EMBT and SHBT models were updated based on the experimental and numerical FRFs to determine the unknown parameters of the composite hollow shaft. Table 2 presents the obtained parameters by the considered optimization process. The numerical and experimental FRFs are showed in Fig. 4a, Fig. 4b, and Fig. 4c.

Figure 3. Detail of the accelerometer placement and the elastic support used during the experimentation.

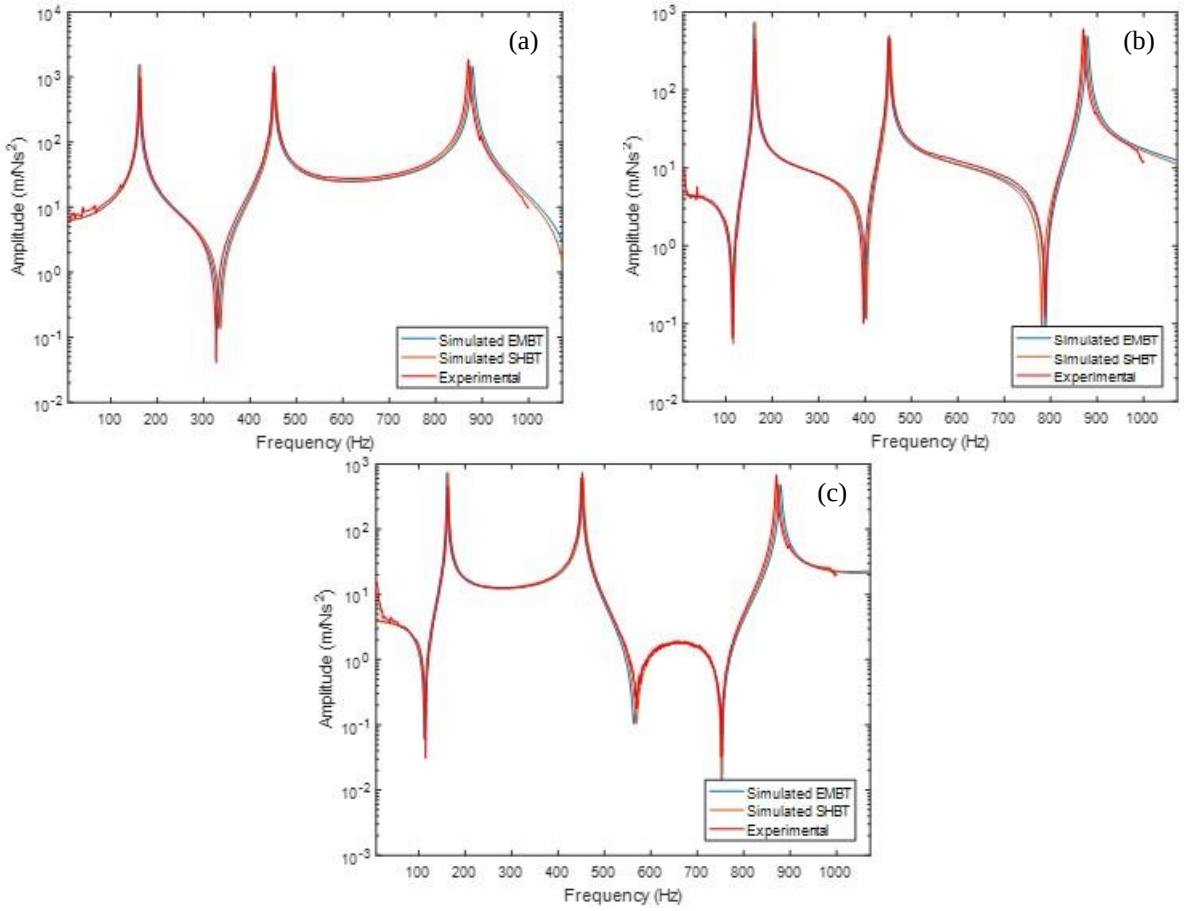

Figure 4. Numerical and experimental FRFs for the sensor position in (a) L=0m, (b) L=0.378m and (c) L=0.529m

Table 2. Design variables used in optimization.

Variable	Minimum limit	Optimized value	Maximum limit
Youngs Modulus 0° [GPa]	90	90.99	91
Youngs Modulus 90° [GPa]	68	68.95	69
Youngs Modulus 0°/90° [GPa]	102	102.93	103
In-Plane Shear Modulus [GPa]	9	10	12
In-Plane Shear Modulus 0°/90° [GPa]	9	11.05	12
Major Poisson's Ratio	0.35	0.39	0.4
Major Poisson's Ratio 0°/90°	0.15	0.17	0.4
η_1	$1x10^{-7}$	$7.42x10^{-4}$	$1x10^{-3}$
η_2	$1x10^{-7}$	$2.791x10^{-4}$	$1x10^{-3}$
η_3	$1x10^{-7}$	$1.461x10^{-4}$	$1x10^{-3}$

As can be seen, the numerical FRFs obtained by both models are satisfactorily close to the experimental data. The result of the SHBT model is most similar to the experimental ones since, differently from the EMBT, it takes into account the stacking sequence into the formulation.

Figure 5 presents the scheme of the rotating machine used in this work. It is worth mentioning that only numerical simulations were performed with the rotor system. The rotating machine is composed of a horizontal composite hollow shaft represented by 39 finite elements (mechanical and geometric properties are showed in Tab. 2) and two rigid steel discs (ρ=7800 kg/m^3), positioned at nodes #13 and #30 with diameter d=0.15m and thickness e=0,02m. The rotor is simply supported (representation of the bearings) at nodes #5 and #36. An unbalance of $1x10^{-5}$Kg.m / 0º applied to the disc was considered.

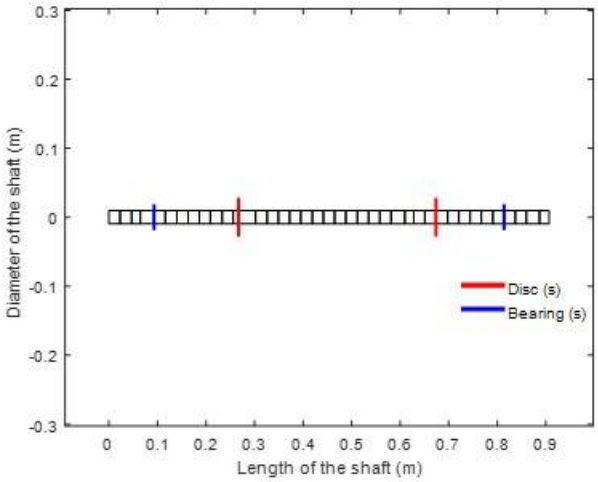

Figure 5. Representation of the rotor

Figure 6 shows the Campbell diagram of the rotor system, obtained from the EMBT and SHBT models. Note that the first forward critical speed obtained by the EMBT model is 1280 rev/min, approximately. The first forward critical speed determined by the SHBT model is 1270 rev/min. The instability threshold can be verified at, approximately, the first forward critical speed in both methodologies. The instability threshold was determined by analyzing the real part of the eigenvalues associated with the vibration modes of the system.

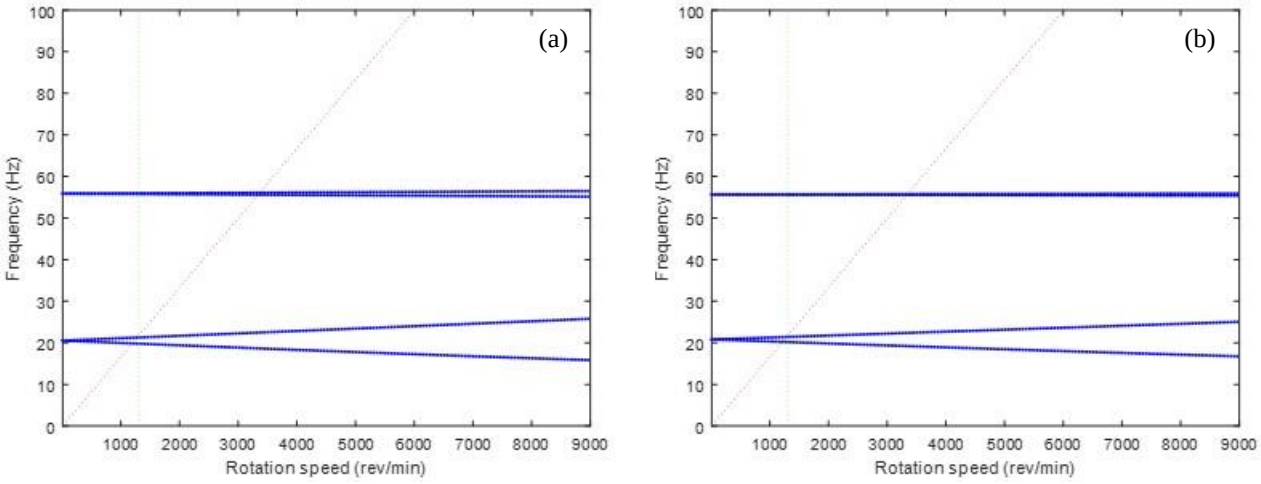

Figure 6. Campbell diagrams of the modeled rotor system obtained from (a) EMBT and (b) SHBT

Figure 7 presents the unbalance responses of the rotor system obtained along the x and z directions at the disc position considering both the EMBT and SHBT models. The rotor system is operating in a run-up condition from 0 to 9000 rev/min in steps of 20 rev/min.

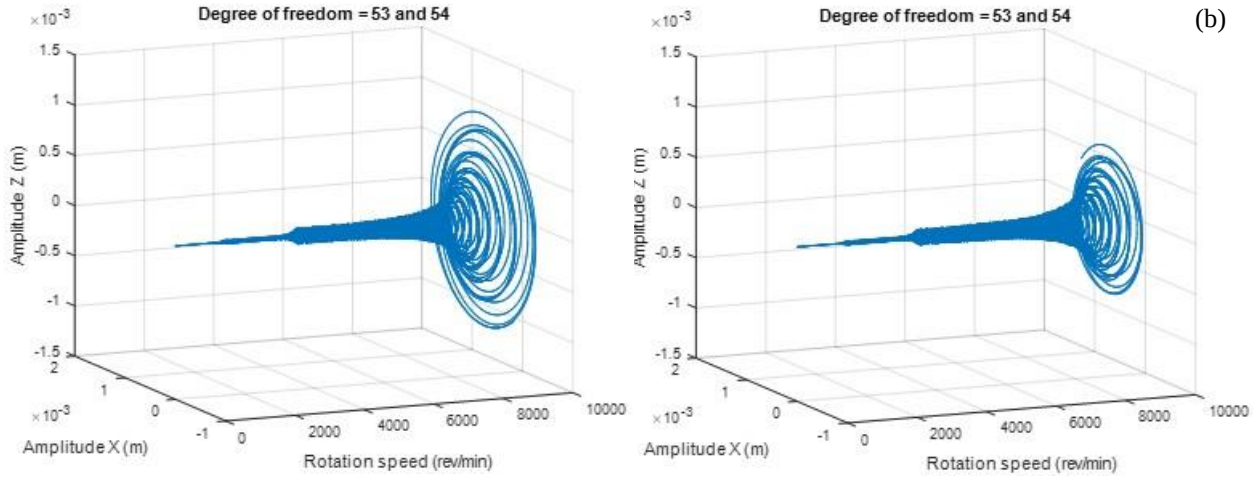

Figure 7. Unbalance responses of the rotor system

As expected, the vibration amplitudes increase for rotation speeds bigger than the instability threshold. The EMBT model shows a higher vibration level as compared with the SHBT model. More in-depth evaluations will be further conducted to evaluate these results.

4. FINAL REMARKS

In this paper, a preliminary investigation regarding the dynamic behavior of a composite hollow shaft was discussed. The mathematical model of the rotor was developed based on established rotordynamic theories and further developed into finite element models, considering both the EMBT and SHBT theories. It is noteworthy that, for both theories, the simplifications used in their formulations allowed for a considerably low computational effort, which can be of great advantage as compared to other approaches, such as plate and shell-based formulations. Experimental tests were performed to determine the unknown parameters of the composite hollow shaft. The optimization procedure was applied to both EMBT and SHBT models. As a result, the physical, geometrical, and mechanical properties of the shaft were determined. Both models have shown a good representation of the experimental results; however, the SHBT model has performed slightly better than the EMBT. This better performance is because the SHBT model considers the composite layers stacking sequence, which has an increasingly prominent effect that is proportional to the shaft wall thickness. This became evident with the experiments performed, as the system considered fall into the category of thick-wall shafts. The rotodynamic behavior was investigated numerically, considering both EMBT and SHBT theories. Similar results were obtained from the two considered approaches. Further research effort encompasses detailed experimental investigations for model validation purposes. For this aim, rotor critical speeds, vibration amplitudes, transient motion, and instability threshold will be evaluated.

5. ACKNOWLEDGEMENTS

The authors are thankful to the Brazilian Research Agencies CAPES, CNPq (574001/2008-5) and FAPEMIG (TEC-APQ-022284-15 / TEC-APQ-307609) for the financial support provided to this research effort.

6. REFERENCES

Brush, M., 1999. *Still Spinning After all These Years – A Profile of The Utracentifuge*, The Scientist, Vol. 13.

Daniel, I.M. and Ishai, O., 1994. *Engineering Mechanics of Composite Materials*. Oxford University Press, New York.

Gupta, K., 2015. "Composite Shaft Rotor Dynamics: An Overview". In: *Sinha, J.K. (Ed.), Vibration Engineering and Technology of Machinery*, Springer. Manchester, p. 79-94.

Lalanne, M. and Ferraris, G., 1998. *Rotordynamics prediction in engineering*. John Wiley & Sons, INC.

Pereira, J.C. and Swider, P., 1997. *Um Elemento Finito Multicamadas Associado a um Modelo de Previsão de Amortecimento*. Congresso Ibero Latino-Americano de Métodos Computacionais para Engenharia – XVIII CILAMCE, Brasília.

Silveira, M.E., 2001. *Análise do Comportamento Dinâmico de Rotores em Eixos Bobinados*. Dissertação de Mestrado. Universidade Federal de Santa Catarina.

Singh, S.P. and Gupta, K., 1994. *Free damped flexural vibration analysis of composite cylindrical tubes using bean and shell theories*. Journal of Sound and Vibration, Vol. 172, p. 171-190.

Sino, R., 2007. *Comportement Dynamique et Stabilite des Rotors: Application aux Rotors Composites*. PhD Thesis, INSA Lyon.

Wattergreen, H. L. and Olsson, K.O, 1996. “Dynamic Instability of a Rotating Asymmetric Shaft with Internal Viscous Damping Supported”. In: Anisotropic Bearings. Journal of Sound and Vibration, Vol. 195, p. 75-84.
Wettergren, H. L., 1997, “Material Damping in Composite Rotors”. In: Journal of Composite Materials, Vol. 32, No. 7/1998, Technomic Publishing Co., Inc.

7. RESPONSIBILITY NOTICE

The authors are the only responsible for the printed material included in this paper.